Localized Gaussian Type Orbital−Periodic Boundary Condition−Density Functional Theory Study of Infinite-Length Single-Walled Carbon Nanotubes with Various Tubular Diameters†

Houng-Wei Wang,‡ Bo-Cheng Wang,*,§ Wen-Hao Chen,§ and Michitoshi Hayashi*,‡,#

Center for Condensed Matter Sciences, National Taiwan University, Taipei 106, Taiwan, Department of Chemistry, Tamkang University, Tamsui 251, Taiwan, and Institute for Molecular Sciences, Okazaki, 444-8585, Japan

Received: May 28, 2007; In Final Form: December 3, 2007

The detailed geometrical structures of zigzag and armchair type single-walled carbon nanotubes (SWCNTs) with infinite tubular length were investigated using localized Gaussian type orbital−periodic boundary condition−density functional theory (LGTO−PBC−DFT) method. The structures of (*n*, 0) zigzag SWCNTs were optimized for $n = 5-21$, (*n*, *n*) armchair SWCNTs for $n = 3-12$. For comparison, the optimized geometry of a two-dimensional graphite sheet was also calculated. It was found that the optimized structures of the SWCNTs showed two C−C bond lengths that decrease with an increase in the tubular diameter. More specifically, the two bond lengths converged with those found in the two-dimensional graphite sheet. We also found a degeneracy in the highest occupied crystal orbitals if identical bond lengths were employed for the zigzag SWCNTs and the two-dimensional graphite sheet. This implies that the two different bond lengths found in the zigzag SWCNTs and the two-dimensional graphite sheet are probably due to the Jahn−Teller effect. The armchair SWCNTs show two slightly different bond lengths if the diameter is less than 12 Å; otherwise they are almost identical, approaching the longer bond length of the two-dimensional graphite sheet. This can be due to the fact that the armchair SWCNTs do not have degeneracy in occupied crystal orbitals for identical C−C bond lengths. The crossing point of the conducting and valence bands of each armchair SWCNT were also calculated and show a diameter dependence in which the deviation from $2\pi/3a$ decreases as diameter increases.

1. Introduction

Carbon nanotubes have attracted considerable attention because of their unique physical properties (elasticity, stiffness, and deformation) and applications in various materials (semiconducting, H_2 storage, and the probes).[1−6] Almost 20 years ago, Smalley et al. discovered a truncated-icosahedral C_{60} carbon cluster by laser vaporization of graphite in a high-pressure supersonic nozzle.[7] In 1991, Ijima detected multiwalled carbon nanotubes in a plasma arc discharge apparatus.[8] Two years later, single-walled nanotubes (SWCNTs) were achieved by Iijima and Bethune. Later, a large-scale purification process was established and the SEM, TEM, and STM characterization of SWCNTs was obtained.[9−11] Although, much scientific interest focused on the physical and electronic properties and commercial applications of these new materials,[11−13] there have been no experimental structural data sufficiently accurate to generate the geometrical structure of isolated SWCNTs. In order to understand the physical properties of SWCNT, theoretical analysis is needed to determine the real nature of SWCNTs and specify their properties.

The geometrical structure of SWCNT is a rolled-up 2-D graphite sheet as a hollow cylindrical shape or a one-by-one layered cyclic carbon array shape as a 1-D tubular axis infinity extension.[14] Defect-free SWCNTs have various types of cylindrical shapes with respect to the array of benzenoids in carbon nanotubes. According to geometrical analysis, there exist armchair, zigzag, and chiral tubules among SWCNTs.

Recently, theoretical and experimental work have predicted that the infinity length SWCNTs are π-bonded aromatic molecules that can be either semiconducting or metallic depending upon the tubular diameter and helical angle.[15,16] In 1992, Saito and Hamada used the tight binding model to generate the band structure of SWCNTs.[17] Almost the same year, Nakamura et al. predicted the infinite length (5, 5) and (6, 6) armchair SWCNT using DFT calculation with plane wave.[18] Recently, the extended tight-binding approximation has been applied to prediction of the optical spectra of SWCNT by Bachilo et al.[19,20] Later, Dresselhaus et al. found that the photoluminescence behavior of SWCNT depends on tube diameter.[21]

For the quantum chemistry calculations, Brus et al. calculated, using DFT, the HOMO−LUMO gaps of finite systems ranging from $C_{20}H_{20}$ to $C_{210}H_{20}$. They extrapolated (5, 5) armchair SWCNT of infinite length from these finite systems. They concluded that (5, 5) armchair SWCNT should show a narrow E_g (energy gap) having a metallic property at infinite length.[15] In a previous work, the semiempirical PM3 method was used to determine the electronic and optimized structures of zigzag and armchair SWCNT with several finite lengths and various tubular diameters.[22]

In order to investigate the infinite system with a periodic unit, the periodic boundary condition (PBC) model has been pre-

† Originally submitted for the "Sheng Hsien Lin Festschrift", published as the September 27, 2007, issue of *J. Phys. Chem. A* (Vol. 111, No. 38).

* Corresponding authors. E-mail: M.H., atmyh@ntu.edu.tw; B.-C.W., bcw@mail.tku.edu.tw.

‡ National Taiwan University.

§ Tamkang University.

Institute for Molecular Sciences.

10.1021/jp074107l CCC: $40.75
Published on Web 02/02/2008

sented that could solve the discrete MO model into continuous bands.[23−26] Thus, one can generate a finite SWCNT segment by using DFT calculation with a Gaussian type molecular orbital and extend it to an infinite length SWCNT model. In 1998, Scuseria et al. used PBC−DFT with localized Gaussian type orbitals (LGTO) to optimize the geometrical structure and to generate the energies of (5, 0) zigzag SWCNTs.[23] Quite recently, Scuseria et al. reported applications of this method with fluorinated SWCNT studies.[27,28] Subsequently, Scuseria's group presented PBC−DFT results of optical transitions in both metallic and semiconducting SWCNTs.[16,29] Thus, the PBC model with LGTO demonstrated a possibility for applications to SWCNTs. Although applications were reported, a more detailed basic structural analysis of SWCNTs is still necessary for a better understanding of the material properties. As far as we know, effects of diameter on a SWCNT structure with high level geometry optimization have not been reported so far. With limited computational resources, most studies used small basis sets such as STO-3G which is a minimal basis set in quantum chemistry calculation. However, it should be important to obtain the geometric details of SWCNTs even for larger diameter tubes using larger basis sets. It is also important to investigate how the diameter depends on geometrical parameters such as the C−C bond lengths and some of the dihedral angles of SWCNTs. In addition, Lin et al. has reported the importance of the effects of curvature and strain of the structure of SWCNTs on the electronic structures using analytic formulation.[30] For a better understanding of the electronic structure of SWCNTs, it is important to obtain a more realistic geometrical structure. Quantum chemistry calculation methods based on LGTO have been established for providing reliable structural information on many molecular systems. Since the SWCNT consists of carbon atoms, LGTO−PBC−DFT is a suitable approach. Therefore, LGTO−PBC−DFT should be performed to determine geometrical and electronic structures of SWCNTs with higher basis sets.

In the present study, we focused on the zigzag and armchair SWCNTs. For comparison, the geometry of two-dimensional graphite sheets was also optimized. LGTO−PBC−DFT calculations were performed on these systems at pure DFT functionals (PBE, VSXC, etc.) levels with 6-31G(d) basis sets after test calculations were carried out using several functionals including hybrid functionals and basis sets. The present paper is organized as follows. In Section 2, we briefly mention the computational details. In Section 3, optimized structures, band structures, and band gaps of the zigzag and those of the armchair SWCNTs are discussed. Our calculated results provide large scale DFT method developers (such as tight-binding DFT) with reliable information and calculation conditions on various zigzag and armchair SWCNTs. Section 4 concludes the present study.

2. Brief Theoretical Background and Calculation Details

The geometrical structure of SWCNT can be described by a chiral vector $\vec{C}_h$ on a two-dimensional graphite sheet where $\vec{C}_h = n\vec{a}_1 + m\vec{a}_2$ with n and m being integers. Here $\vec{a}_1$ and $\vec{a}_2$ represent the unit vectors of the hexagonal honeycomb lattice. SWCNT is a one-dimensional system so that the lattice vector $\vec{T}$ can be defined along the tubule axis and normal to the chiral vector $\vec{C}_h$. Conveniently, SWCNT is presented by a (n, m) pair of numbers; (n, *0*) and (n, n) that designate the zigzag and armchair types SWCNTs, respectively. The carbon atoms of the zigzag SWCNT are arranged as *cis*-polyenes with a single circular of carbon atoms. On the other hand, the armchair SWCNT is obtained by rolling up hexagons in a σ_v symmetry

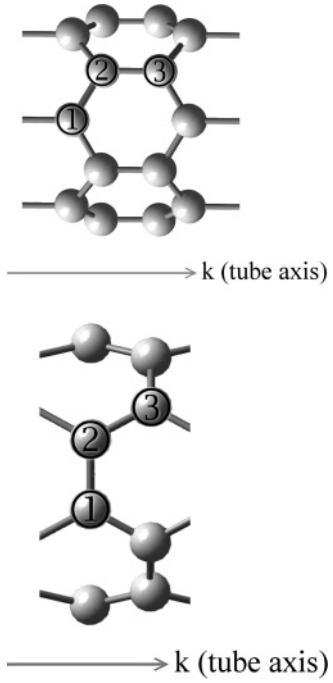

Figure 1. A definition of C−C bonds in (n, 0) zigzag and (n, n) armchair SWCNTs. Panels a and b show the unit structures of the zigzag and armchair SWCNTs, respectively. In each panel two C−C bonds are indicated.

plane such that the carbon atoms are arranged as *trans*-polyenes with a single circular plane of carbon atoms. For the zigzag type SWCNT, n denotes the number of benzenoids in the circumference of the tube, and the translation axis is the *trans*-polyene rings along the tubular length. The tubular diameter (d_{tub}) of (n, 0) zigzag SWCNT can be determined: $d_{tub} = 2r\cos(\pi/6)/\sin(\pi/n)$ where r is the length of the C−C bond in the SWCNT. For the (n, n) armchair SWCNT, $d_{tub} = r/\sin(\pi/3n)$.

For the PBC−DFT calculation of SWCNTs, we started with the single layer for the unit cell and extended it along the tubular axis to infinite length by the PBC model. Panels a and b in Figure 1 show the atomic arrangement of the unit cell for zigzag and armchair SWCNTs, respectively. For example, the unit cell of (5, 0) SWCNT contains 20 carbon atoms for a single circumference; thus, we used these 20 carbon atoms for the starting unit, extending to the infinite tube in this calculation. Note that in each panel in Figure 1 two distinctive carbon−carbon bonds are shown. The PBC−DFT method was implemented in the Gaussian 03 revision C.02 program package.[31] The PBC model in the Gaussian 03 package is based on Gaussian type orbitals (GTOs)[25] that are transformed "crystalline orbitals (CO)" by employing the Bloch function,[32] and then the energy per unit cell can be computed by several algorithms.[23,24,33,34] In the Gaussian 03 program, a redundant internal coordinate algorithm for optimization of periodic systems was developed by Kudin et al.[35] For high precision geometry optimization, extremely tight optimization convergence criteria was used, and ultrafine was chosen for the integral grid option, i.e., (99, 590) grid.

Similar to the HOMO and LUMO of a finite system, the highest occupied crystalline orbital (HOCO) and the lowest unoccupied crystalline orbital (LUCO) can be defined. In this case, the energy gap between the energy of HOCO and that of LUCO corresponds to the band gap, and thus we use the definition given by $E_g = E_{LUCO} - E_{HOCO}$.

We carried out several test calculations to examine the performance and efficiency of various functionals and basis sets

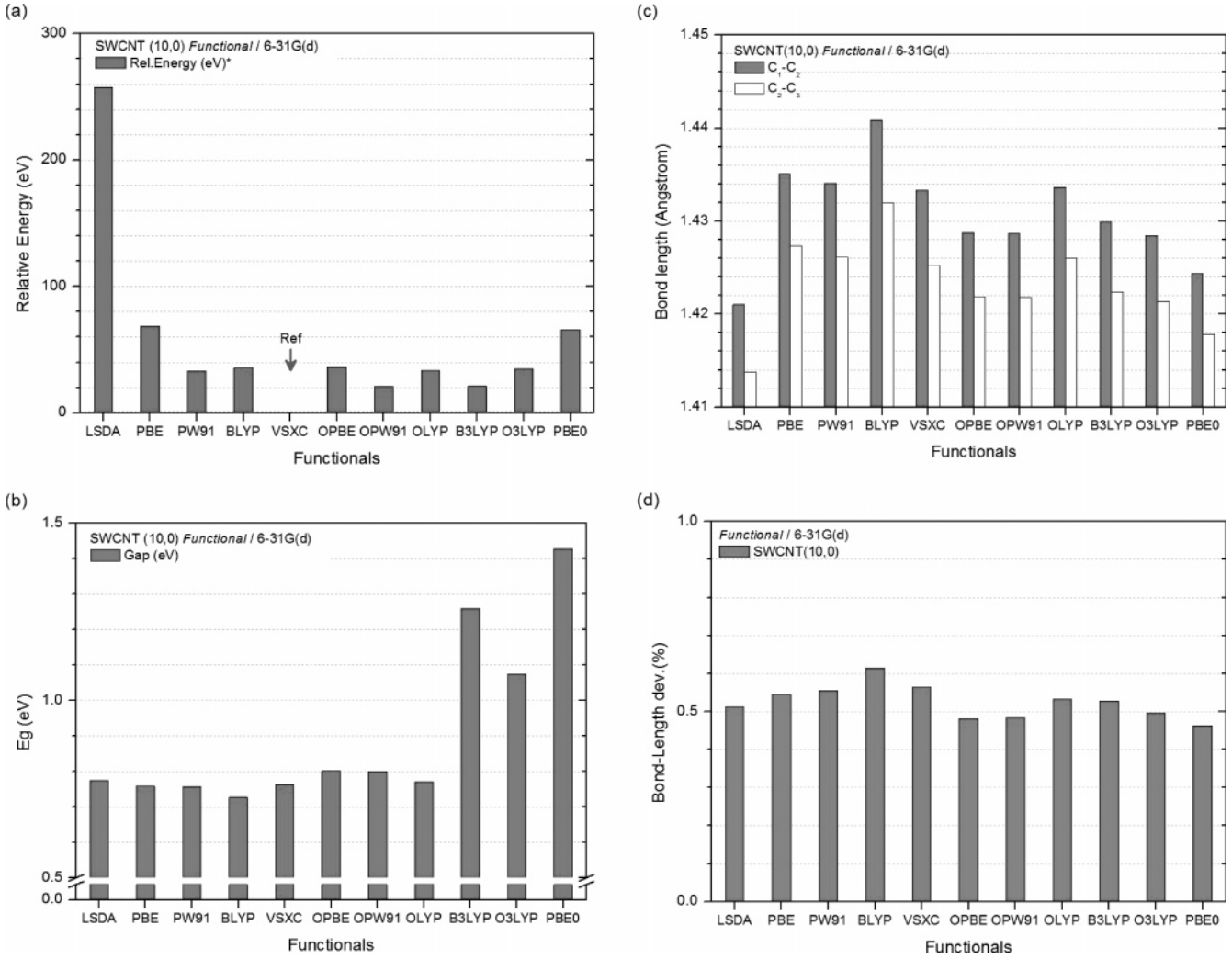

Figure 2. Functional dependency of the calculated properties of (10, 0) zigzag SWCNT. Panels a, b, c, and d show the relative total energy, band gap energy, bond length, and bond length deviation related to the two bond lengths shown in panel c, respectively. The relative energy is defined as the difference between a calculated total energy of the current method and the lowest total energy in all used methods. Panel c and d clearly show that there are two apparently different bond lengths in the (10, 0) zigzag SWCNT.

with the LGTO−PBC−DFT method. For this purpose, we optimized the geometry of (10, 0) zigzag SWCNT with various types of functionals (LSDA, PBE, PW91, BLYP, VSXC, B3LYP, etc.) using 6-31G(d) basis set, and the corresponding total energy and band gap energies were computed. Figure 2 shows the calculated results. Panels a and b in Figure 2 show that the VSXC[36] functional gives the lowest total energy and a relatively larger energy gap compared with those calculated with LSDA,[37] PBEPBE,[38] PW91PW91,[39] BLYP,[40,41] VSXC, OPBE,[38,42] OPW91,[39,42] OLYP,[41,42] B3LYP,[41,43] O3LYP,[44] and PBE0.[45] B3LYP and OPW91 functionals predict a total energy quite close to that calculated with VSXC, but the band gap by B3LYP is different from the other functionals as shown in Figure 2(b). The optimized bond lengths for various functionals are shown in panels c and d in Figure 2. It is obvious that there are two different bond lengths in (10, 0) SWCNT. Functionals PBEPBE, PW91PW91, OLYP, and VSXC predict similar bond lengths among them while B3LYP, OPBE, and OPW91 form another group. BLYP and LSDA predict quite different bond lengths; BLYP somehow gives the largest bond length and LSDA the smallest.

The basis set effects were also examined using eight basis sets: STO-3G, 3-21G, 6-31G, 6-31G(d), 6-311G, 6-311G(d), 6-31+G(d), and 6-311+G(d) with VSXC functional. The geometry of (10,0) SWCNT was optimized with each basis set. The computed results are shown in Figure 3. The total energy shows a strong basis set dependence while the band gap energy convergence is achieved at 6-31G(d) as shown in panels a and b in Figure 3. The calculated bond lengths of varies basis sets are also shown in panels c and d in Figure 3. We find that the bond length difference is also converged at the 6-31G(d) basis set. Basis sets larger than 6-31G(d) consume considerable computational resources. Thus, we adopted 6-31G(d) as a more reasonable choice for tradeoff of the computing resources for the following calculations. Note that the geometrical structure optimized using STO-3G largely deviates from the others. Compared with 6-31G(d), STO-3G-calculated results show a 1.3% deviate in the average bond lengths and the rest are ±0.2%.

From the above calculation results together with Scuseria's report,[23] we used the VSXC functional and 6-31G(d) basis set for the geometry optimization and band structure calculations of the zigzag and armchair SWCNTs. We also examined effects of *k*-points on the band gap and geometrical structure of SWCNTs. The calculated results show that the number of *k*-points has no effect on the band gap or structure of the zigzag SWCNTs. Thus, the 79 *k*-points (G03 package autosetting value) are used in all calculations for the zigzag SWCNT. The band gaps of the armchair SWCNTs, on the other hand, depend strongly on the number of *k*-points. After several tests, we set

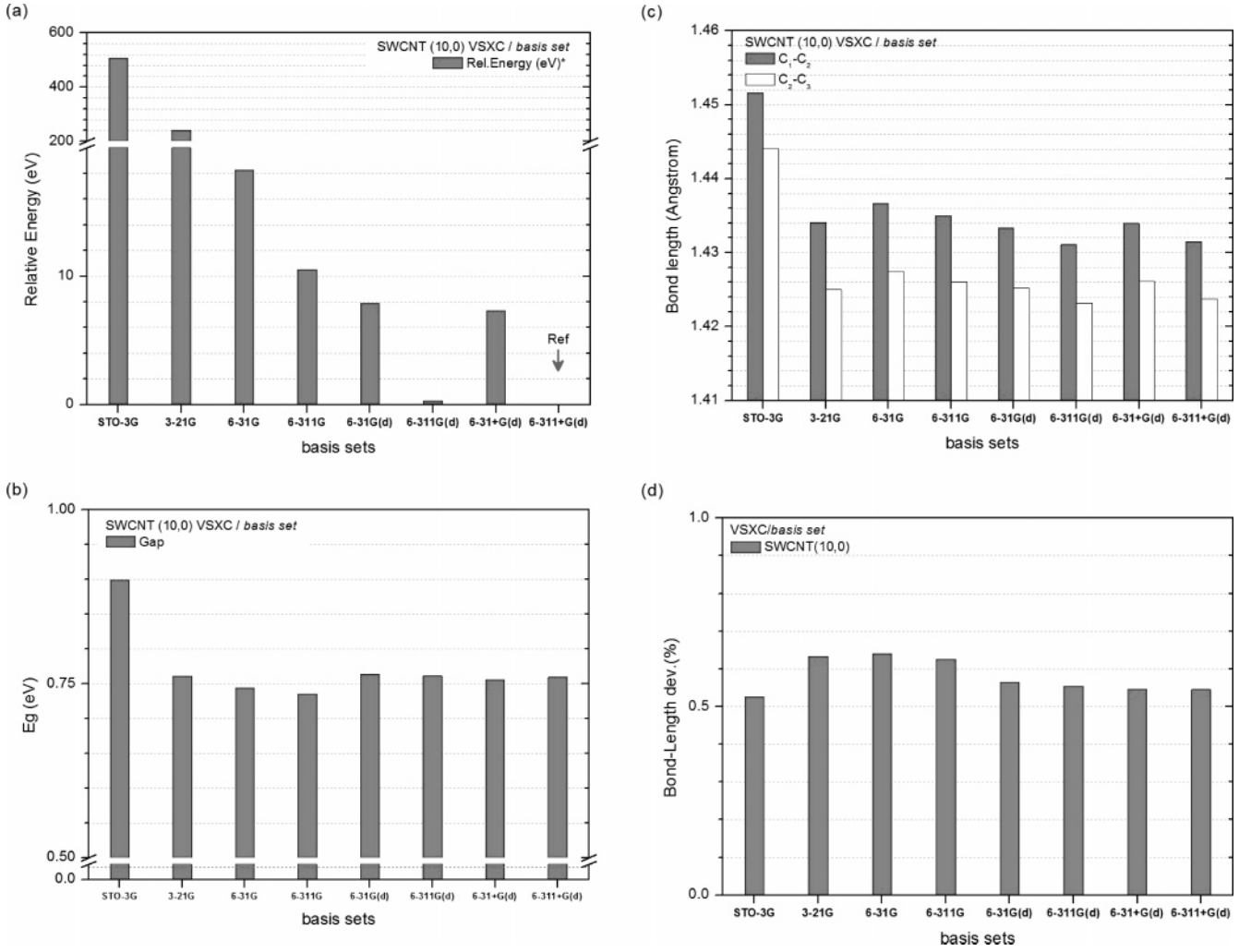

Figure 3. Basis set dependences of the calculated properties of (10, 0) zigzag SWCNT. Panels a, b, c, and d show the relative total energy, band gap energy, bond length, and bond length deviation, respectively. Panel b and d show the energy gap and the bond lengths are converged at 6-31G(d) basis set.

2192 *k*-points (137 × 16, where 137 is the G03 package autosetting value) for armchair SWCNTs.

3. Results and Discussion

3.1. Zigzag Type SWCNT. On the basis of the structure analysis, we consider the zigzag SWCNT to consist of *n* number of benzenoids in the circumference of the tube. Thus, the minimum unit contains one-layer benzenoid structure in the circumference of the tube. We optimized geometries of zigzag SWCNTs for various tubular diameters from (5, 0) to (21, 0) and computed their corresponding band structures.

Table 1 presents the geometrical parameters and tubular diameter calculated using PBC−DFT for the infinite length zigzag SWCNTs. The calculated tubular diameters increase from 4.022 Å for (5, 0) SWCNT to 16.545 Å for (21, 0) SWCNT; there is nearly a 0.8 Å tubular diameter difference between any two neighboring SWCNTs.

Although tight-binding methods with LDA methods were employed to investigate large size SWCNTs, they assumed that SWCNT has the same C−C bond length in the entire nanotube system.[17,46] In the present study, the C−C bond lengths of SWCNT were optimized to two different values that are probably closer to a real carbon tube structure than other methods. According to Table 1, (6, 0) SWCNT has two different C−C bond lengths: 1.449 Å and 1.413 Å. As the diameter increases, the two C−C bond lengths of the optimized structure becomes very close; for example, the (13, 0) SWCNT has 1.430 Å and 1.427 Å. The difference between the two lengths is almost constant for the (14, 0) through (21, 0) SWCNTs. This tendency can be easily seen in Figure 4 in which bond length deviation (%) = bond length difference/bond length average × 100 is calculated for various *n*. Figure 4 clearly shows that the bond length has an oscillatory feature with a period of 3. Our computational results imply that an increase in the tubular diameter of the infinite zigzag SWCNTs leads to more delocalization of π electrons so that the tubular diameter does not affect the C−C bond length larger than (13, 0) SWCNT. Thus, the SWCNTs ($n \geq 13$) can be regarded as a nearly rolled-up graphite sheet. We will discuss this feature later with armchair SWCNTs. Furthermore, the calculated geometric structure of (5, 0) SWCNT shows a distorted structure from cylinder symmetry. In this case, we found that the bond lengths are distributed in a wide range so that the bond length average of C_1-C_2 or C_2-C_3 is less significant. For example, the standard deviations of the C_1-C_2, and C_2-C_3 bond lengths are the largest among all calculated zigzag SWCNTs and they are 0.02581 and 0.02103, respectively, while the corresponding standard deviations of (6, 0) SWCNT, for example, are 0.00040 and 0.00073.

Table 1 also lists the calculated E_g of an infinite length (*n*, 0) zigzag SWCNT. The calculated E_g exhibits oscillation

TABLE 1: Calculated Geometrical Parameters and Electronic Structures (HOCO, LUCO, and E_g) for (n, 0) Zigzag SWCNTS by VSXC/6-31G(d) Calculation Level with PBC Method

(n, 0) n =	diameter (Å)	C_1-C_2 (Å)[a]	C_2-C_3 (Å)[a]	HOCO	LUCO	E_g (eV)
5	4.022	1.459	1.409	−4.8534	−4.8532	0.0002[b]
6	4.792	1.449	1.413	−4.0890	−4.5331	0.0014[b]
7	5.557	1.440	1.422	−4.4539	−4.2495	0.2044
8	6.345	1.439	1.420	−4.5061	−3.8664	0.6398
9	7.127	1.436	1.422	−3.9827	−3.8360	0.1467
10	7.902	1.433	1.425	−4.3604	−3.5959	0.7645
11	8.693	1.433	1.424	−4.3823	−3.4192	0.9632
12	9.475	1.432	1.425	−3.9757	−3.9079	0.0678
13	10.256	1.431	1.426	−4.2926	−3.6573	0.6353
14	11.046	1.431	1.425	−4.3112	−3.5662	0.7450
15	11.830	1.430	1.426	−3.9793	−3.9405	0.0388
16	12.612	1.430	1.427	−4.2534	−3.7104	0.5429
17	13.402	1.430	1.426	−4.2597	−3.6565	0.6032
18	14.187	1.430	1.426	−3.9819	−3.9591	0.0228
19	14.970	1.429	1.427	−4.2167	−3.7499	0.4668
20	15.760	1.429	1.427	−4.2260	−3.7162	0.5098
21	16.545	1.429	1.427	−3.9871	−3.9707	0.0164

[a] The position of carbon atoms shown in Figure 1(a). [b] k-points = 1264.

TABLE 2: Calculated Geometrical Parameters and Electronic Structures (HOCO, LUCO, and E_g) for (n, n) Armchair SWCNTs by VSXC/6-31G(d) Calculation Level with PBC Method

(n, n) n =	diameter (Å)	C_1-C_2 (Å)[a]	C_2-C_3 (Å)[a]	HOCO	LUCO	E_g
3	4.122	1.440	1.437	−3.9182	−3.8889	0.0294
4	5.480	1.435	1.433	−3.8926	−3.8887	0.0040
5	6.837	1.432	1.431	−3.9138	−3.9121	0.0017
6	8.196	1.431	1.430	−3.9325	−3.9292	0.0033
7	9.559	1.430	1.429	−3.9467	−3.9445	0.0022
8	10.921	1.430	1.429	−3.9554	−3.9551	0.0003
9	12.282	1.429	1.429	−3.9643	−3.9633	0.0010
10	13.643	1.429	1.429	−3.9705	−3.9696	0.0009
11	15.006	1.429	1.428	−3.9760	−3.9744	0.0016
12	16.368	1.428	1.428	−3.9812	−3.9799	0.0013

[a] The position of carbon atoms shown in Figure 1(b).

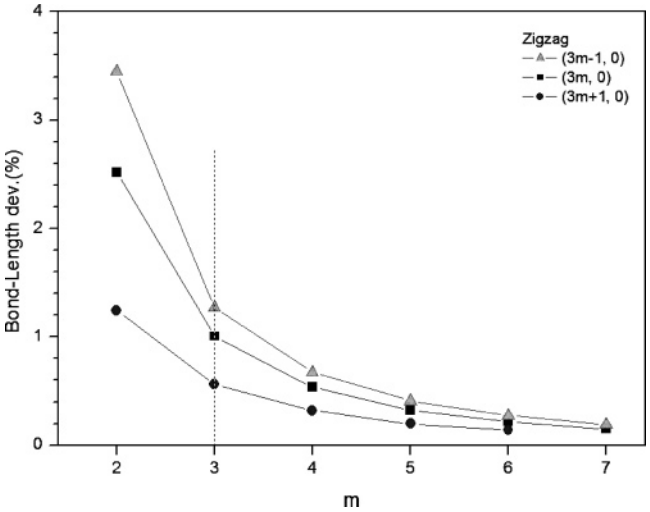

Figure 4. Calculated bond length deviation for (n, 0) zigzag SWCNTs ($5 \le n \le 21$). In order to see a periodicity in bond length deviation (or bond length), the bond length deviations are plotted as a function of the integer m with which (n, 0) zigzag SWCNTS are presented as ($3m - 1$, 0), ($3m$, 0), and ($3m + 1$, 0).

properties with the repeat unit having $n = 3m$, $3m + 1$, and $3m + 2$, where m is 2, 3, 4, 5, 6 (for all series), and 7 (only for $n = 3m$ series). One can see that the largest band gap is obtained for the ($n = 3m + 2$, 0) SWCNTs while the ($n = 3m$, 0) SWCNTs have the smallest in each $\Delta n = 3$ section. The calculated E_g values for the (6, 0), (9, 0), (12, 0), (15,0), (18, 0), and (21, 0) SWCNTs are 0.0002 eV, 0.1467 eV, 0.0678 eV, 0.0387, 0.0228, and 0.164 eV, respectively. For the (7, 0), (10, 0), (13, 0), (16, 0), and (19, 0) SWCNTs, the calculated E_g are 0.2044 eV, 0.7645 eV, 0.6353, 0.5429, and 0.4668 eV, respectively. Thus, our calculation results at this level indicate that (n, 0) SWCNTs with n being a multiple of 3 have a small band gap energy very close to those experimentally observed.[47] Obviously, the others have a semiconducting character. The calculation results also suggest that (8, 0), (11, 0), (14, 0), (17, 0), and (20, 0) SWCNTs have the largest band gap in each $\Delta n = 3$ section.

We compared our results with the other calculation results. For this purpose, we chose (7, 0) and (13,0) SWCNTs whose E_g are 0.2044 and 0.6353 eV in the present study, respectively. Ito et al. reported $E_g = 0.1304$ eV for GGA (PW91) and 0.1943 eV for LDA with plane wave functions.[46] Very early, the calculated E_g by the tight-binding model was reported to be 0.14 eV for this SWCNT.[17] Our calculation is much closer to that of the LDA results. Hamada et al. used the tight-binding model to calculate E_g for (13, 0) SWCNT, and the value is 0.697 eV,[17] which is also consistent with the present study.

It is informative to show the band structures of the zigzag SWCNTs. Panel a in Figure 5 presents the calculated HOCO and LUCO energies at Γ point and the corresponding band gap energies. For example, the calculated HOCO and LUCO bands for (10, 0) SWCNT are −4.3603 eV and −3.5960 eV, and the energy gap is 0.7643 eV. Panel b in Figure 5 shows the band structures calculated for the (5, 0), (6, 0), (8, 0), (10, 0), (16, 0), and (21, 0) zigzag SWCNTs.

3.2. Armchair Type SWCNT. Table 2 lists the optimized geometrical parameters, calculated HOCO and LUCO energies, and energy gap (E_g) of armchair SWCNTs. Note that the calculated tubular diameters vary from 4.122 Å for (3, 3) to

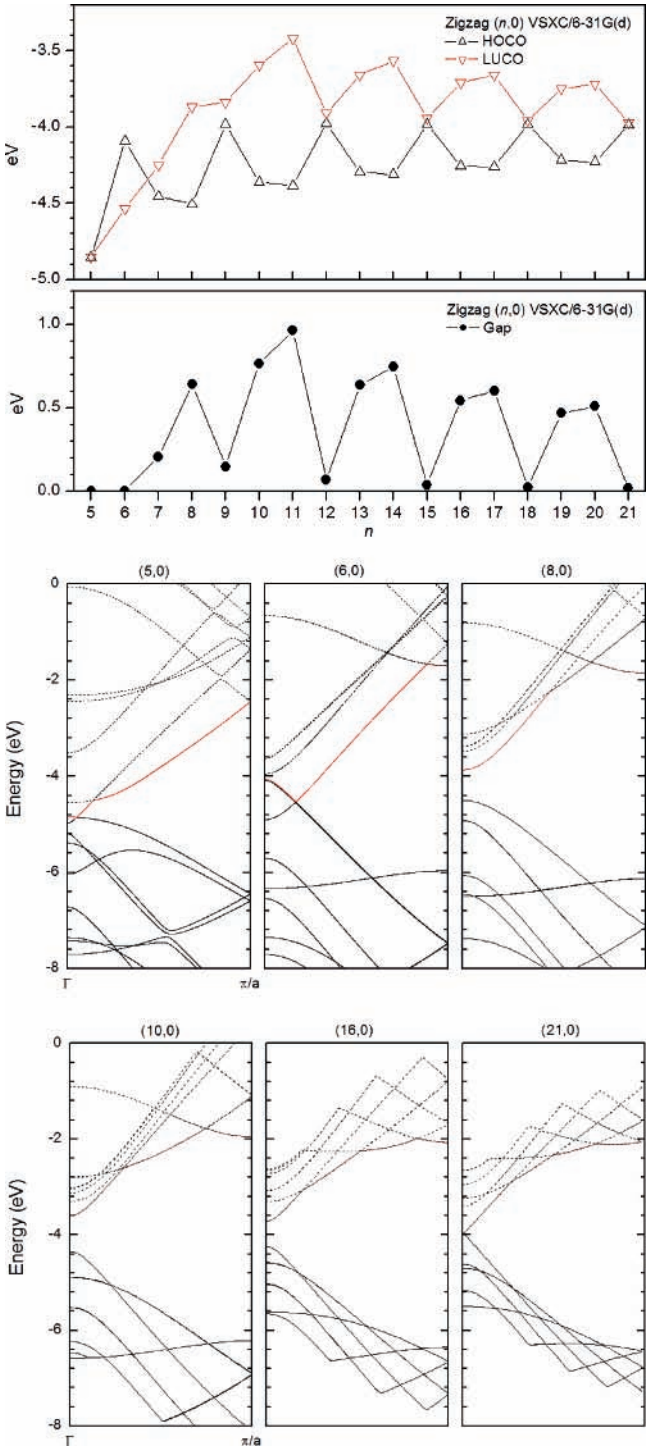

Figure 5. Calculated HOCO and LUCO energies, band gaps, and band strictures of zigzag SWCNTs. HOCO and LUCO energies and band gaps of (n, 0) zigzag SWCNTs ($5 \leq n \leq 21$) are shown in panel a, and band structures of (5,0), (6,0), (8,0) (10,0), (16,0), and (21,0) zigzag SWCNTs are presented in panel b. (5,0) and (6,0) zigzag SWCNTs are shown because they deviate from the series shown in the lower figure in panel a.

16.368 Å for (12, 12). There are almost no differences between two C−C bond lengths in armchair SWCNTs when $n > 4$. For the (3, 3) armchair SWCNT, the smallest tube diameter causes the bond length slightly longer to maintain the tubular geometry. This leads the properties of this SWCNT to be slightly different from other armchair series. For the (4, 4) armchair SWCNT, two slightly different bond lengths 1.435 Å and 1.433 Å are found in the optimized structure. Apparently, the difference of

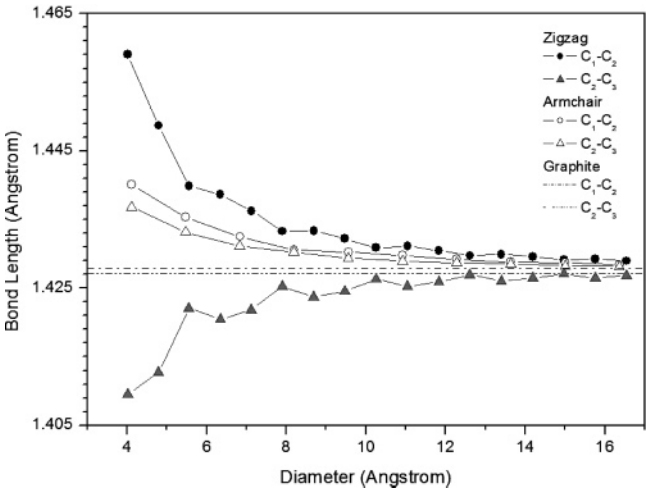

Figure 6. Comparison of the calculated bond lengths of various sizes of zigzag and armchair SWCNTs. The calculated bond length of a two-dimensional graphite sheet is also shown as the limiting case.

the two C−C bond lengths decreases with increasing n, approaching an identical bond length (1.42788 Å) at the (12, 12) SWCNT.

Figure 6 compares the bond lengths of the zigzag and armchair SWCNTs. The zigzag SWCNTs clearly show an oscillatory feature in the bond lengths with a period of 3 as mentioned earlier while the armchair SWCNTs do not exhibit such a trend. In addition, the two bond lengths of the zigzag SWCNTs show drastic changes as the diameter increases; the shorter one increases and the longer one decrease. On the other hand, the two bond lengths of each armchair SWCNT decrease with increasing diameter even after the two become identical. The results shown in Figure 6 suggest that zigzag and armchair SWCNTs may have an identical bond length at much larger diameters.

For comparison, we optimized the geometry of the two-dimensional graphite sheet. It was found that two different bond lengths exist in the optimized structure, and they are 1.42719 Å and 1.42788 Å. It is very interesting that the two bond lengths of the zigzag SWCNTs approach these two bond lengths at larger diameters. Now a question arises: why do the C−C bond lengths of a zigzag SWCNT with a large diameter (>16 Å) approach those of the two-dimensional graphite sheet while an armchair conveys identical bond lengths? In the limiting case in which the diameter is infinitely long, can the C−C bonds of the zigzag and armchair SWCNTs asymptotically be regarded as those of a graphite sheet? To answer this question, we examined if there was any degeneracy in the crystal orbitals of these systems. We found that there is degeneracy in the highest occupied crystal orbitals for of a two-dimensional graphite sheet if identical bond lengths are used. Interestingly, a similar degeneracy was also found in the highest occupied crystal orbitals of the zigzag SWCNTs if identical bond lengths are employed. Note that the symmetrical structures of the SWCNTs and graphite sheet are not the optimized geometries. Moreover, there is no degeneracy in the occupied crystal orbitals of the armchair SWCNT ((12, 12) for instance) with a symmetrical geometry. The optimized structure is almost symmetric; standard deviations of bond lengths and dihedral angles are less that 0.0001 and 0.25, respectively. The above-mentioned results imply that the two different bond lengths found in the zigzag SWCNTs and the two-dimensional graphite sheet are probably due to the Jahn−Teller effect while armchair SWCNTs can allow very symmetric structures at larger diameters.

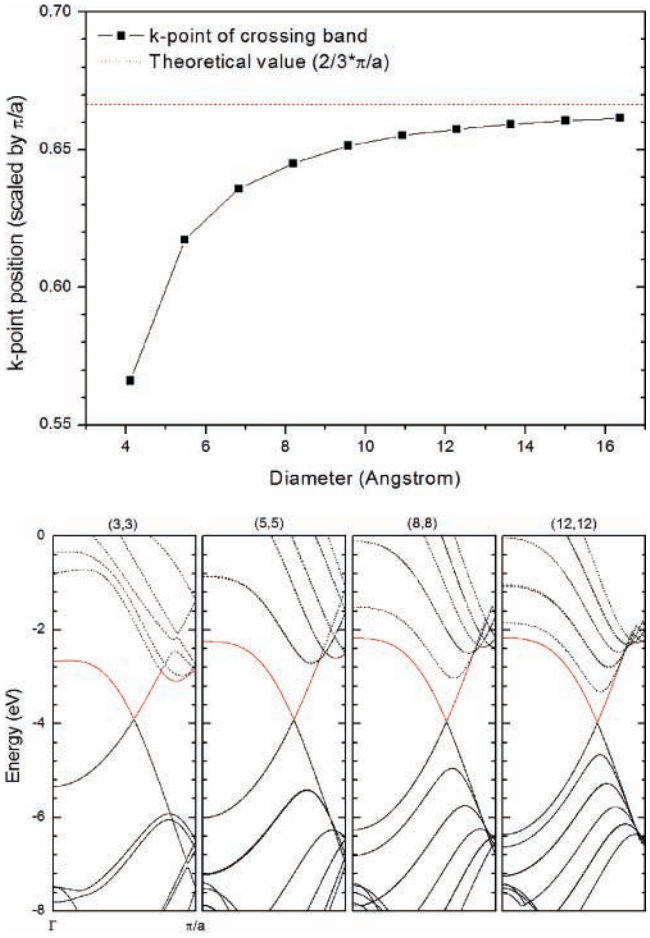

Figure 7. Crossing k-points of (n, 0) armchair SWCNTs as a function of radius. A theoretical value $2/3 \times \pi/a$ based on symmetric structure model (an identical bond length for all C−C bonds) is shown in panel a. As the diameter increases the crossing k-points approach this value. Band structures of several armchair SWCNTs are shown in panel b.

It is also informative to examine the band structures of the armchair SWCNTs based on the optimized structures and the HOCO and LOCO energies crossing the point along $k = |\vec{k}|$ since each armchair SWCNT with a different radius has different optimized geometrical parameters. In this case, the crossing points should depend on the geometries. We define k_c as the value at which the HOCO and LOCO energies have a crossing point. Panel a of Figure 7 shows k_c as a function of the diameter of the optimized armchair SWCNT. As is anticipated, k_c exhibits a diameter dependence, and in addition, we also find that the value approaches $2/3 \times \pi/a$ that is obtained for an armchair SWCNT with homogeneous C−C bond lengths and lattice constant a. The band structures of (3, 3), (5, 5), (8, 8), and (12, 12) armchair SWCNTs are also presented in panel b of Figure 7 as examples of the results.

4. Conclusion

In this study, we investigated the geometrical and electronic structures of zigzag and armchair types of SWCNT with the infinite tubular length using LGTO−PBC−DFT method at VSXC level with 6-31G(d). The major difference in the bond lengths of the optimized zigzag and armchair SWCNTs is that the C−C bonds of the zigzag SWCNTs at a large diameter can be regarded as those of a two-dimensional graphite sheet while those of the armchair SWCNTs cannot. The occupied crystal orbital analysis suggests that the Jahn−Teller effect probably plays an important role in the difference.

It is well-known experimentally that the tubular diameters of SWCNTs can vary, ranging from 10 Å to 16 Å with a peak maximum at 12 Å.[48] The present calculation shows that the diameters of (15, 0), (16, 0), and (9, 9) SWCNTs are around 12 Å; thus, these can be the most possible products. The geometrical properties calculated in this work provide important information needed for a design of new nanoelectronic devices or a detailed understanding of excited states of SWCNTs.

Acknowledgment. We thank the National Science Council of ROC for support. One of the authors (M.H.) thanks the NSC for financial support (NSC-95-2113-M-002-027-MY3) and National Taiwan University for financial support (95R0066-23), and the National Center for High-performance Computing in Hsinchu for providing access to the computational resources.

Supporting Information Available: Calculated geometrical parameters; curvatures of armchair SWCNTs. This material is available free of charge via the Internet at http://pubs.acs.org.

References and Notes

(1) Ajayan, P. M.; Stephan, O.; Colliex, C.; Trauth, D. *Science* **1994**, *265*, 1212.
(2) Saito, Y.; Hamaguchi, K.; Hata, K.; Uchida, K.; Tasaka, Y.; Ikazaki, F.; Yumura, M.; Kasuya, A.; Nishina, Y. *Nature* **1997**, *389*, 554.
(3) deHeer, W. A.; Chatelain, A.; Ugarte, D. *Science* **1995**, *270*, 1179.
(4) Collins, P. G.; Zettl, A.; Bando, H.; Thess, A.; Smalley, R. E. *Science* **1997**, *278*, 100.
(5) Nardelli, M. B.; Yakobson, B. I.; Bernholc, J. *Phys. Rev. B* **1998**, *57*, R4277.
(6) Huang, J. Y.; Chen, S.; Ren, Z. F.; Chen, G.; Dresselhaus, M. S. *Nano Lett.* **2006**, *6*, 1699.
(7) Kroto, H. W.; Heath, J. R.; O'.; Brien, S. C.; Curl, R. F.; Smalley, R. E. *Nature* **1985**, *318*, 162.
(8) Iijima, S. *Nature* **1991**, *354*, 56.
(9) Iijima, S.; Ichihashi, T. *Nature* **1993**, *363*, 603.
(10) Bethune, D. S.; Kiang, C. H.; deVries, M. S.; Gorman, G.; Savoy, R.; Vazquez. J.; Beyers, R. *Nature* **1993**, *363*, 605.
(11) Ouyang, M.; Huang, J. L.; Lieber, C. M. *Acc. Chem. Res.* **2002**, *35*, 1018.
(12) Kane, C. L.; Mele, E. J. *Phys. Rev. Lett.* **1997**, *78*, 1932.
(13) Hartschuh, A.; Pedrosa, H. N.; Peterson, J.; Huang, L.; Anger, P.; Qian, H.; Meixner, A. J.; Steiner, M.; Novotny, L.; Krauss, T. D. *Chem. Phys. Chem.* **2005**, *6*, 577.
(14) Hamada, N.; Sawada, S.; Oshiyama, A. *Phys. Rev. Lett.* **1992**, *68*, 1579.
(15) Zhou, Z. Y.; Steigerwald, M.; Hybertsen, M.; Brus, L.; Friesner, R. A. *J. Am. Chem. Soc.* **2004**, *126*, 3597.
(16) Barone, V.; Peralta, J. E.; Wert, M.; Heyd, J.; Scuseria, G. E. *Nano Lett.* **2005**, *5*, 1621.
(17) Saito, R.; Fujita, M.; Dresselhaus, G.; Dresselhaus, M. S. *Phys. Rev. B* **1992**, *46*, 1804.
(18) Matsuo, Y.; Tahara, K.; Nakamura, E. *Org. Lett.* **2003**, *5*, 3181.
(19) Bachilo, S. M.; Strano, M. S.; Kittrell, C.; Hauge, R. H.; Smalley, R. E.; Weisman, R. B. *Science* **2002**, *298*, 2361.
(20) Weisman, R. B.; Bachilo, S. M. *Nano Lett.* **2003**, *3*, 1235.
(21) Samsonidze, G. G.; Saito, R.; Kobayashi, N.; Grüneis, A.; Jiang, J.; Jorio, A.; Chou, S. G.; Dresselhaus, G.; Dresselhaus, M. S. *Appl. Phys. Lett.* **2004**, *85*, 5703.
(22) Wang, B. C.; Wang, H. W.; Lin, I. C.; Lin, Y. S.; Chou, Y. M.; Chiu, H. L. *J. Chin. Chem. Soc.* **2003**, *50*, 939.
(23) Kudin, K. N.; Scuseria, G. E. *Chem. Phys. Lett.* **1998**, *289*, 611.
(24) Kudin, K. N.; Scuseria, G. E. *Phys. Rev. B* **2000**, *61*, 16440.
(25) Erkoç, S. *Int. J. Modern Phys. C* **2000**, *11*, 547.
(26) Cao, H.; Ma, J.; Zhang, G. L.; Jiang, Y. S. *Macromolecules* **2005**, *38*, 1123.
(27) Kudin, K. N.; Bettinger, H. F.; Scuseria, G. E. *Phys. Rev. B* **2001**, *63*, 045413.
(28) Bettinger, H. F.; Kudin, K. N.; Scuseria, G. E. *J. Am. Chem. Soc.* **2001**, *123*, 12849.
(29) Barone, V.; Peralta, J. E.; Scuseria, G. E. *Nano Lett.* **2005**, *5*, 1830.
(30) Li, T. S.; Lin, M. F. *Phys. E* **2006**, *33*, 57.
(31) Gaussian 03, Revision C.02, Frisch, M. J.; Trucks, G. W.; Schlegel, H. B.; Scuseria, G. E.; Robb, M. A.; Cheeseman, J. R.; Montgomery, J. A., Jr.; Vreven, T.; Kudin, K. N.; Burant, J. C.; Millam, J. M.; Iyengar, S. S.; Tomasi, J.; Barone, V.; Mennucci, B.; Cossi, M.; Scalmani, G.; Rega, N.; Petersson, G. A.; Nakatsuji, H.; Hada, M.; Ehara, M.; Toyota, K.; Fukuda,

R.; Hasegawa, J.; Ishida, M.; Nakajima, T.; Honda, Y.; Kitao, O.; Nakai, H.; Klene, M.; Li, X.; Knox, J. E.; Hratchian, H. P.; Cross, J. B.; Bakken, V.; Adamo, C.; Jaramillo, J.; Gomperts, R.; Stratmann, R. E.; Yazyev, O.; Austin, A. J.; Cammi, R.; Pomelli, C.; Ochterski, J. W.; Ayala, P. Y.; Morokuma, K.; Voth, G. A.; Salvador, P.; Dannenberg, J. J.; Zakrzewski, V. G.; Dapprich, S.; Daniels, A. D.; Strain, M. C.; Farkas, O.; Malick, D. K.; Rabuck, A. D.; Raghavachari, K.; Foresman, J. B.; Ortiz, J. V.; Cui, Q.; Baboul, A. G.; Clifford, S.; Cioslowski, J.; Stefanov, B. B.; Liu, G.; Liashenko, A.; Piskorz, P.; Komaromi, I.; Martin, R. L.; Fox, D. J.; Keith, T.; Al-Laham, M. A.; Peng, C. Y.; Nanayakkara, A.; Challacombe, M.; Gill, P. M. W.; Johnson, B.; Chen, W.; Wong, M. W.; Gonzalez, C.; and Pople, J. A.; Gaussian, Inc., Wallingford, CT, 2004.

(32) Pisani, C., Ed. *Lecture Notes in Chemistry*; Springer-Verlag: Heidelberg, 1996; Vol. 67.

(33) Feibelman, P. J. *Phys. Rev. B* **1987**, *35*, 2626.

(34) Jaffe, J. E.; Hess, A. C. *J. Chem. Phys*. **1996**, *105*, 10983.

(35) Kudin, K. N.; Scuseria, G. E. *J. Chem. Phys.* **2001**, *114*, 2919.

(36) Voorhis, T. V.; Scuseria, G. E. *J. Chem. Phys.* **1998**, *109*, 400.

(37) Vosko, S. H.; Wilk, L.; Nusair, M. *Can. J. Phys*. **1980**, *58*, 1200.

(38) Perdew, J. P.; Burke, K.; Ernzerhof, M. *Phys. Rev. Lett*. **1997**, *78*, 1396.

(39) Perdew, J. P.; Burke, K.; Wang, Y. *Phys. Rev. B* **1996**, *54*, 16533.

(40) Becke, A. D. *Phys. Rev. A* **1988**, *38*, 3098.

(41) Lee, C.; Yang, W.; Parr, R. G. *Phys. Rev. B* **1988**, *37*, 785.

(42) Handy, N. C.; Cohen, A. J. *Mol. Phys*. **2001**, *99*, 403.

(43) Becke, A. D. *J. Chem. Phys*. **1993**, *98*, 5648.

(44) Cohen, A. J.; Handy, N. C. *Mol. Phys.* **2001**, *99*, 607.

(45) Perdew, J. P.; Burke, K.; Ernzerhof, M. *Phys. Rev. Lett*. **1996**, *77*, 3865.

(46) Ito, T.; Nishidate, K.; Baba, M.; Hasegawa, H. *Surf. Sci.* **2002**, *514*, 222.

(47) Ouyang, M.; Huang, J. L.; Cheung, C. L.; Lieber, C. M. *Science* **2001**, *292*, 702.

(48) Rinzler, A. G.; Liu, J.; Dai, H.; Nikolaev, P.; Huffman, C. B.; Rodríguez-Macías, F. J.; Boul, P. J.; Lu, A. H.; Heymann, D.; Colbert, D. T.; Lee, R. S.; Fischer, J. E.; Rao, A. M.; Eklund, P. C.; Smalley, R. E. *Appl. Phys. A* **1998**, *67*, 29.